ArF Lasers for Production of Semiconductor Devices with CD < 0.15 μm

T.P. Duffey, T. Embree, T. Ishihara, R. Morton, W.N. Partlo, T. Watson, R. Sandstrom

Cymer, Inc., 16750 Via del Campo Ct, San Diego, CA 92127

ABSTRACT

The present day notion of the extensibility of KrF laser technology to ArF is revisited. We show that a robust solution to ArF requirements can be met by significantly altering the laser's core technology– discharge chamber, pulsed power and optics. With these changes, a practical ArF tool can be developed. Some of the laser specifications are:

Bandwidth:	0.6 pm (FWHM) 1.75 pm (95% Included Energy)
Average Power:	5 W
Repetition Rate:	1000 Hz
Energy Stability (3σ):	20% (burst mode) 8% (continuous)
Pulse Width:	25 ns

Keywords: DUV lithography, ArF Excimer laser, line-narrowing, 193 nm

1. INTRODUCTION

The transition of laser-based Deep UV lithography systems, employing KrF excimer lasers operating at 248 nm, into mass production of integrated circuits has directed increased attention to development of the next-generation lithography light source: ArF excimer lasers operating at 193 nm. Current projections are that 193 nm sources will be required for fabrication of semiconductor devices with critical dimensions of less than 0.15 μm.[1,2]

The perception exists within the lithography community that ArF laser performance is unalterably and significantly inferior to that of KrF systems, particularly with regard to average power, energy stability, and system reliability. An alternate position is that, while certain physical disadvantages are evident—lower gain, shorter upper state lifetime, increased optical damage—in a comparison between the ArF and KrF laser transitions, intelligent engineering can produce a design that mitigates these factors greatly. Noting the rapid evolution in ArF laser performance in recent years,[3,4] a reasonable projection is that ArF laser development will parallel that of KrF, with a time lag that will decrease as KrF technology matures.

This paper describes the design and performance of a prototype ArF laser system, designated ELX-5000A, consolidating a number of design improvements which permit 5 W average power at 1 kHz operation, with 0.6 pm bandwidth (FWHM). The data in this paper were acquired under normal operation during a system life test, at a point when the system had accumulated 600 Mshots.

Optical Microlithography XI, Luc Van den Hove, Editors,
Proceedings of SPIE Vol. 3334 (1998) · 0277-786X/01/$15.00

2. SYSTEM CONFIGURATION

1. Optics Modules

The ArF laser described herein is based on a Cymer ELS-5000 series KrF laser frame, employing identical modules for gas handling, cooling, AC distribution and system control. The fundamental optical design of the laser is also similar to the ELS-5000, and is depicted in Figure 1. The optical cavity is comprised of:

i) a gas discharge chamber possessing angled windows to reduce reflection losses and assist polarization selection
ii) a partially transmitting mirror for an output coupler, and
iii) a line-narrowing module employing a diffraction grating in the Littrow configuration as a rear reflector with intracavity apertures for wavelength selection/discrimination; an anamorphic beam expander between the rear aperture and the grating enhances the dispersive effect of the grating.

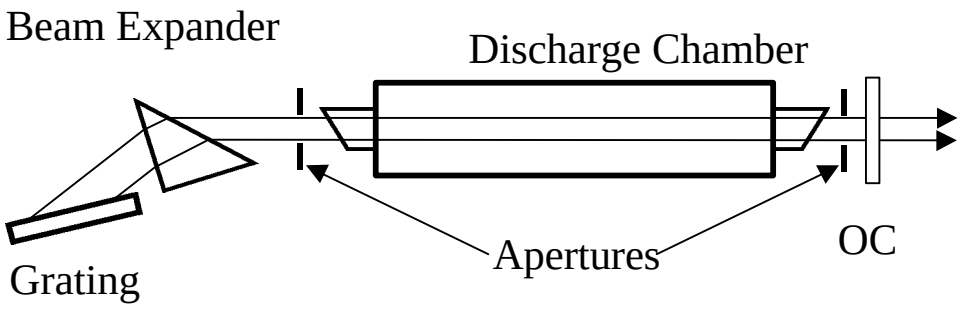

Figure 1. Optical cavity of spectrally-narrowed ArF laser

Details of the line narrowing package (LNP) design vary between the 248 nm and 193 nm packages. Most significantly, the coatings and/or substrates of all optical components have been changed for improved performance and lifetime at 193 nm operation. Similarly, the stabilization module, which measures center wavelength, bandwidth and pulse energy, employs optical components selected for 193 nm use.

2. Pulse Power

The solid state pulse power module for the ELX-5000A incorporates several modifications from that used in the ELS-5000. First of these is the use of a high voltage supply with increased dynamic range (550-950 V) and faster charging rate permitting use of the full dynamic range at 1 kHz repetition rate. Second, this voltage is stepped-up by a factor of 28X rather than 20X. Finally, a redesigned voltage compression stage reduces the risetime of the high voltage pulse delivered to the discharge peaking capacitors. The net result of these changes is the ability to deliver more energy to the gain medium with a 30% reduction in rise time, improving the gain efficiency.

3. Chamber

The discharge chamber is substantially different from a standard KrF chamber. The basic chamber geometry and electrodes were redesigned for improved efficiency. Changes in the preionization scheme and electric field distribution eliminate downstream arcing at 1 kHz repetition rates, reducing rolloff in

average power with increasing repetition rate. Replacement of elastomers by metal seals, and substitution of other materials within the chamber improve gas life and efficiency. Finally, the composition of the gas fill was altered for improved passive gas life. Typical operating pressure is 380 kPa, with a (nominal) 0.1% F_2 concentration.

3. REPETITION RATE

Figure 2 displays typical average power as a function of pulse repetition rate. The data is taken at 100% duty cycle at constant HVPS voltages (INT HV mode) of 700, 800 and 900 V. Maximum voltage the system permits is 950 V. For the 800 and 900 V curves, the rolloff in energy is approximately 20% at 1 kHz. At duty cycles typical of lithography application (40-70%), the operating voltage range for 5 mJ output at 1 kHz is 710-750 V. The considerable headroom in average power permits significant extension of chamber life.

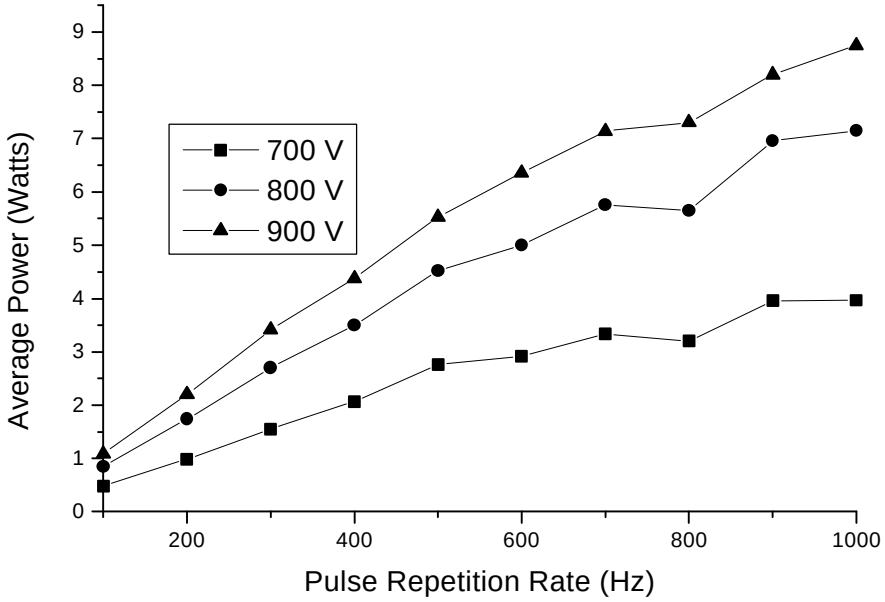

Figure 2. Average Power vs. Repetition rate. 100% duty cycle, fully line-narrowed.

4. SPECTRUM

Correction of chromatic aberration in imaging systems becomes very challenging at 193 nm, due to the high dispersion of the few optical materials suitable for use at this wavelength. Thus, the need for narrow spectral bandwidth is critical. For these considerations, the full width half maximum (FWHM) width is not an entirely reliable measure of the spectral quality. A better formula is the width of the spectral band which includes 95% of the beam energy (95% integral), which better accounts for energy in the wings of the distribution. Figure 3 shows a time-averaged spectrum for a laser operating at 5 mJ/pulse, 1 kHz repetition rate with a 67% duty cycle (0.5 sec firing, 0.25 sec pause). A 20X y-axis magnification of the spectrum is superimposed on the graph to better display the character of the spectral wings. FWHM bandwidth (deconvolved) was measured at 0.42 pm using a 193 nm grating spectrometer manufactured by Cymer. The slit function of this instrument is 0.15 pm. The 95% integral, calculated from the spectrum before deconvolution, was measured at 1.05 pm. Increasing pulse energy to 7.5 mJ using the same burst sequence increased the FWHM value only slightly, to 0.43 pm, while the 95% integral increased by roughly 25%, to 1.30 pm. Figure 4 displays the spectral data for 7.5 mJ output. These results demonstrate that improvement in output power via an increase in laser efficiency (i.e. higher pulse energy) is possible without a large sacrifice in spectral properties.

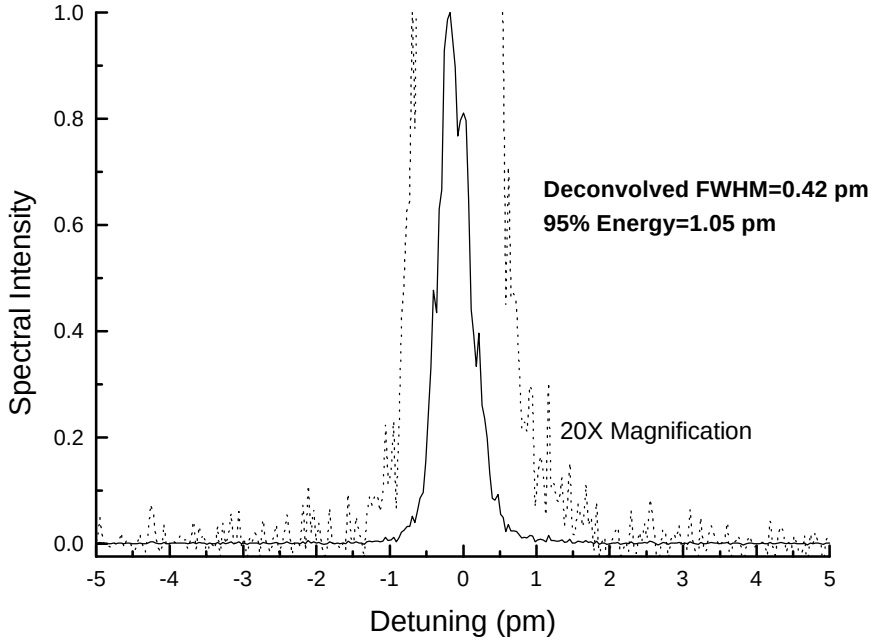

Figure 3. Time-averaged spectrum of laser operating in Internal Energy mode at 5 mJ, 1 kHz operation, 67% duty cycle. The dashed line shows the wings of the spectrum magnified by a factor of 20.

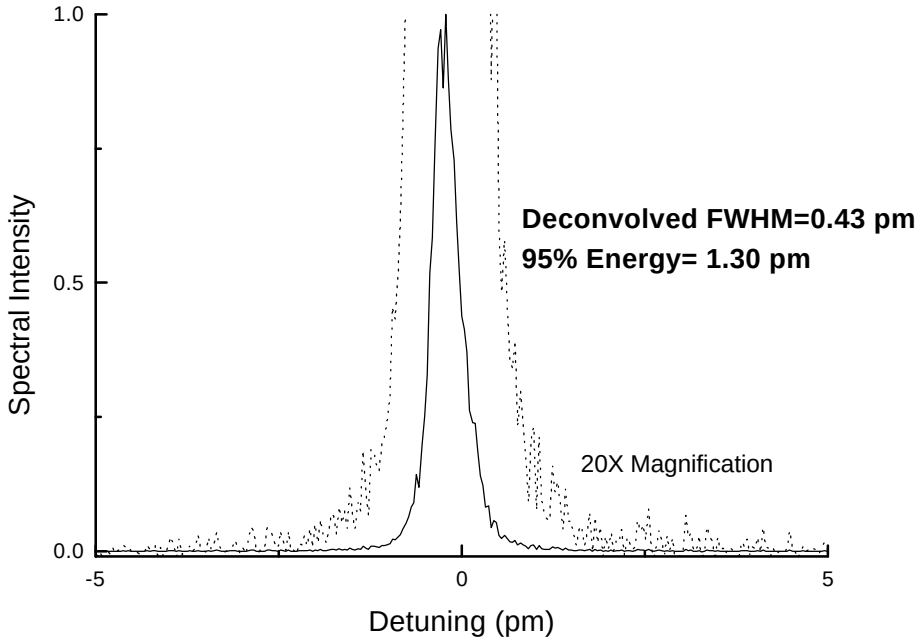

Figure 4. Time-averaged spectrum of laser operating in Internal Energy mode at 7.5 mJ, 1 kHz operation, 67% duty cycle. The dashed line shows the wings of the spectrum magnified by a factor of 20.

5. ENERGY STABILITY

Efficient exposure of photoresist requires that the laser exhibit excellent dose stability. Figure 5 displays a histogram of the maximum and minimum deviations within each burst, from a target dose of 0.15 J (30 pulses), in a sequence of 2000 bursts, 125 pulses/burst at 1 kHz repetition rate. That is, for each burst, the maximum and minimum dose, using a 30-pulse sliding window, was recorded. These values form the data set for the histogram shown in Fig 6. Hence, all doses in this 2000-burst sequence were within 1.1% of the target. The energy values are obtained from the laser's internal Energy Monitor diagnostic.

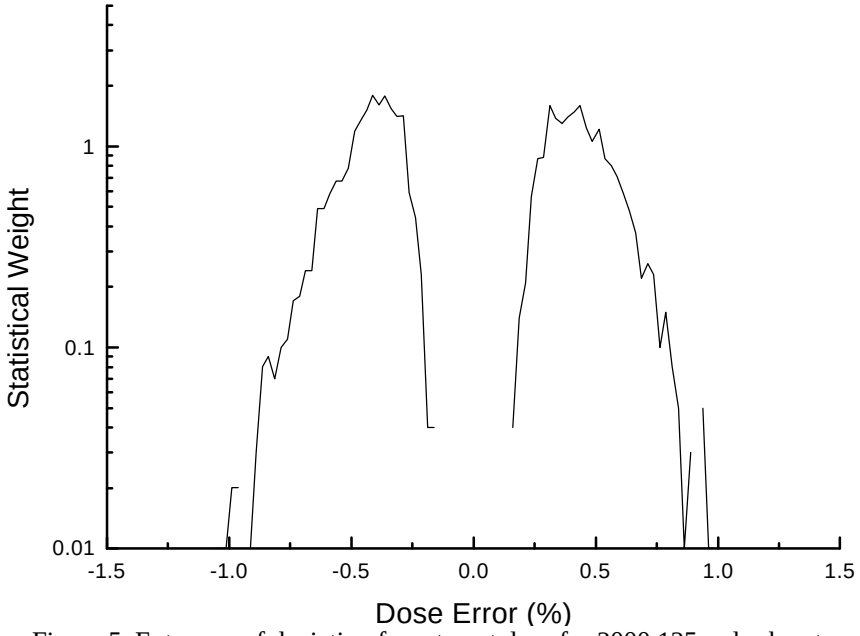

Figure 5. Extremes of deviation from target dose for 2000 125-pulse bursts. Energy setpoint at 5 mJ/pulse, 1 kHz repetition rate.

Figure 6 shows a different analysis of the same sequence of 2000 bursts: a measurement of the 3σ of the energy distribution as a function of pulse number in the burst. The value is less than 20% in all cases; for continuous operation, the number is 8%.

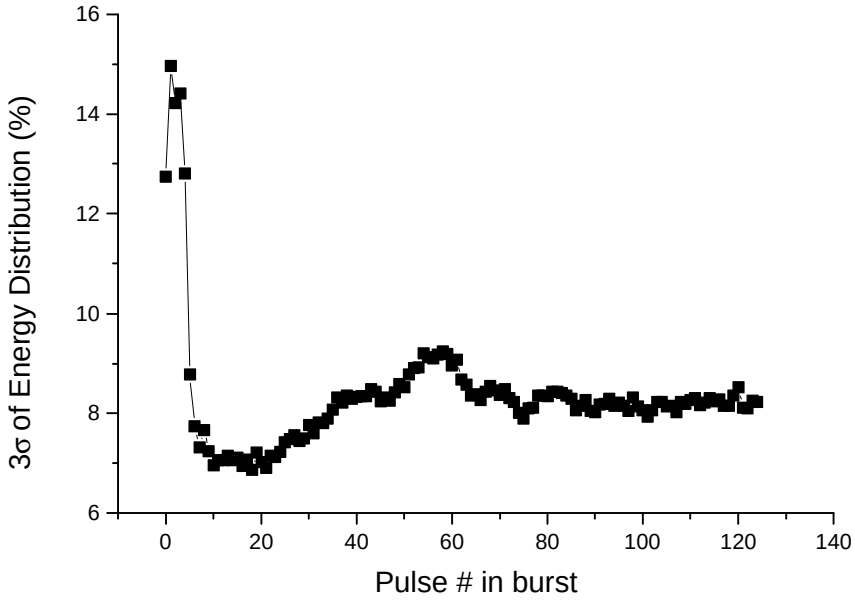

Figure 6. 3σ of energy vs. Pulse number. Same operating conditions as in Figure 5.

6. PULSE WIDTH

The temporal shape of the optical pulse is a major concern in 193 nm lithography applications because of its impact on peak power, and hence, optical damage to transmissive elements in the beam line. Because both compaction (for fused silica)[5] and color center formation via two photon absorption (fused silica and CaF_2) have a nonlinear dependence on peak power, Figure 7 shows the temporal pulse for the ELX5000A. The operating conditions were 5 mJ at 1 kHz continuous firing (100% duty cycle). The signal was collected using a biplanar vacuum photodiode and a fast oscilloscope, and renormalized so that the y-axis values give the peak power, which is slightly greater than 0.2 MW. Two pulse width values are given: the full width half maximum value of 29.1 ns, and the integral-squared pulse width, defined[6] as:

$$t_{I-Sq} = \frac{\left(\int I(t)dt\right)^2}{\int I^2(t)dt}$$

The integral-squared pulse width is a better measure of the pulse's capacity for optical damage, since it tends to suppress the effects of extremely narrow, high amplitude features appearing in the temporal profile. Such features, though having high power values, contain little total energy to effect optical damage. In contrast, the FWHM value could be fully determined by a such a feature, giving an erroneous impression of a very damaging pulse. The integral-squared pulse width is 39.6 ns. Both the FWHM value and the integral-squared value are more than 2X improvements over recently reported values.[3] The pulse width varies by as much as 20% over the 20 million shot gas life of the laser, mostly due to changes in the fluorine concentration due to consumption by the discharge and periodic small injections of the fluorine-bearing gas mix.

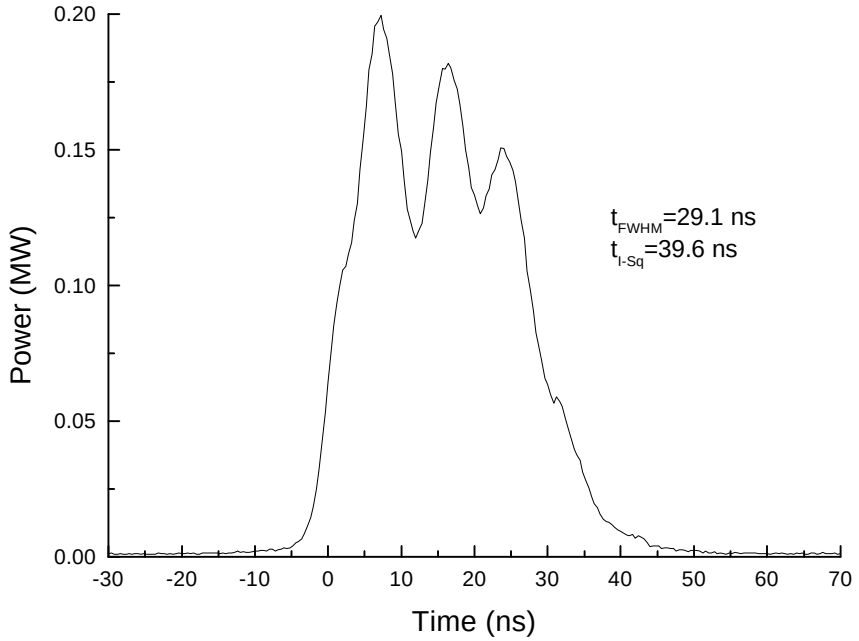

Figure 7. Pulse shape: Peak power vs. time.

7. LIFE TEST

At present, chamber life is the most significant issue in assessing cost of ownership of the ArF system. Complete data on chamber life is not yet available. Figure 8 shows a subset of data from a lifetest, depicting superimposed graphs of FWHM bandwidth and operating voltage at the end of gas life. It is apparent from this graph that end-of-life has not been reached at the 600 Mshot level. Chamber and pulse power design are undergoing rapid development to extend the chamber lifetime.

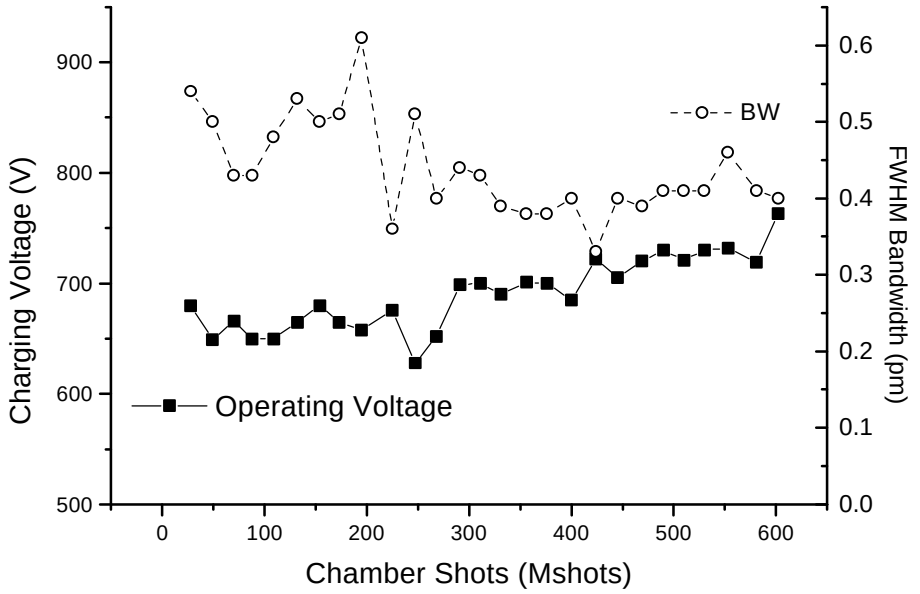

Figure 8. Chamber life test data. 380 kPa gas fill.
Operating conditions: 5 mJ at 1 kHz, 500 pulses/burst.

8. CONCLUSION

We have demonstrated a fully line-narrowed prototype ArF laser suitable for process development in 193 nm lithography applications. The laser has excellent spectral characteristics, and good energy stability. Pulse widths have been extended considerably, minimizing optical damage concerns. Work is underway to evaluate and extend module life, as well as increase average power and repetition rate. The rapid development in these areas suggests that when 193 nm lithography becomes a production process, ArF lasers can exhibit performance not significantly inferior to KrF systems.

9. REFERENCES

1. T. Farrell, R. Nunes, D. Samuels, et al, "The challenges of 1 Giga-bit DRAM development when using optical lithography", *Proc. SPIE*, vol. 3051, pp. 333-341, 1997.
2. M. Levenson, "Wavefront engineering from 500 nm to 100 nm CD", *Ibid*, pp. 2-13.
3. Richard Sandstrom, "Performance data for a sub-1 pm line-narrowed argon fluoride laser for DUV lithography", *Proc. of the SEMI Technology Symposium'97*, printed separately, 1997.
4. U. Stamm, J. Kleinschmidt, P. Heist, I. Bragin, R. Patzel, D. Basting, "ArF excimer laser for 193 nm lithography", *Proc. SPIE*, vol. 3051, pp.868-873, 1997.
5. Richard Schenker, F. Piao, W.G. Oldham, "Durability of experimental fused silicas to 193-nm-induced compaction,", *Ibid*, pp.44-45.
6. Richard Sandstrom, *Proc. of 2nd Symposium on 193 nm Lithography*, Colorado Springs, CO, 1997.